Electronic Supplementary Information

Oxide-supported Rh catalysts for H_2 generation from low-temperature ethanol steam reforming: Effects of support, Rh precursor and Rh loading on catalytic performance

Lin Huang,* Catherine Choong, Luwei Chen, Zhan Wang, Ziyi Zhong, Kee Ann Chng and Jianyi Lin*

Institute of Chemical and Engineering Sciences, Agency for Science, Technology and Research, 1 Pesek Road, Jurong Island, Singapore 627833, Singapore
Fax: (+65)-6316-6182
E-mail: huang_lin@ices.a-star.edu.sg (L. Huang); LiJY@ntu.edu.sg (J. Lin)

XRD analysis of MgO derived from $Mg(OH)_2$

Fig. 1 shows the XRD pattern change after 4 h of calcination of $Mg(OH)_2$ in air at 400 °C. Evidently, the pattern in Fig. 1(a) due to $Mg(OH)_2$ (*Physicochem. Probl. Miner. Process,* 2012, **48,** 631-643) disappeared and a new pattern in Fig. 1(b) assigned to MgO (*Appl. Catal. A.,* 2000, **198,** 33-41) appeared, which indicates the structural transition after the calcination.

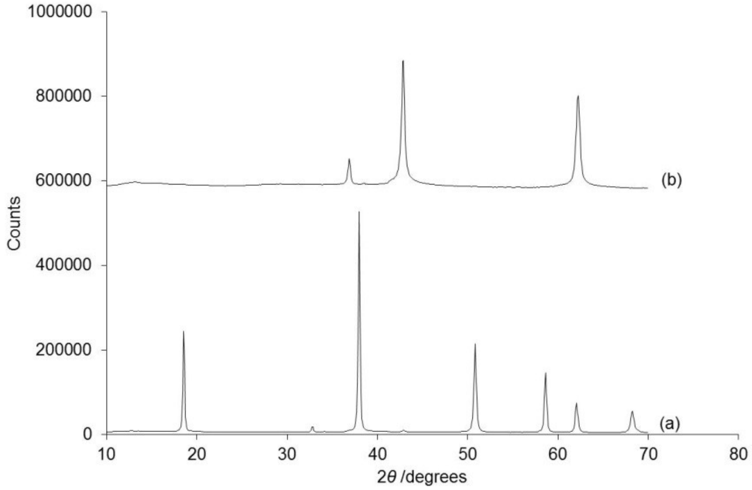

Fig. 1 XRD patterns of $Mg(OH)_2$ (a) before and (b) after 4 h of calcination in air at 400 °C.

TPR pertinent to CeO_2 and Rh precatalysts

$Rh_4(C)/CeO_2$ In the cases where CeO_2-supported Rh precatalysts are made from zero-valent Rh carbonyls, the resulting Rh in the precatalysts remains zero-valent.[33] It is usually unlikely to observe any Rh reduction signals in the TPR of the precatalysts. Hence we oxidized such Rh precatalysts as $Rh_4(C)/CeO_2$ in air at 21 °C for 5 h and at 110 °C overnight before TPR experiments, in order to study the reductive behaviour of the oxidized Rh on CeO_2.

CeO_2 and $Rh^{3+}(N)/CeO_2$ Fig. 2 shows the TPR patterns of CeO_2 alone and $Rh^{3+}(N)/CeO_2$ following 2 h of drying in vacuum (10^{-2} torr) at 21 °C. Similar to a reported TPR result of commercial low-surface-area CeO_2,[74] the TPR pattern of our commercial low-surface-area CeO_2 displayed two shoulder peaks near 540 and 645 °C below 800 °C. In the TPR pattern of $Rh^{3+}(N)/CeO_2$, these two shoulder peaks decreased in intensity in favour of the appearance of a very weak peak centred at 380 °C, which would result from the shoulder peak shift to lower temperatures for the reduction of surface Ce^{4+} due to H spillover from Rh to the support. Since $Rh^{3+}(N)/CeO_2$ has not undergone any calcination pretreatments, the Rh^{3+}-CeO_2 interaction is very weak. On the other hand, the surface area of our CeO_2 is very low. Therefore, the observed H spillover effect is negligible in terms of TPR peak intensity.

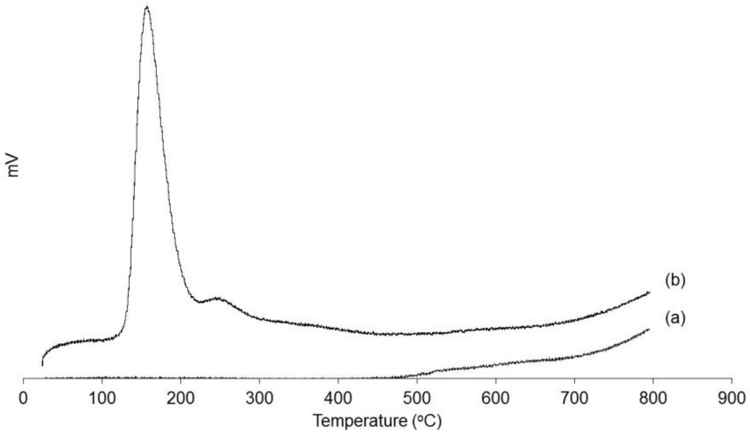

Fig. 2 TPR profiles of (a) CeO_2 and (b) $Rh^{3+}(N)/CeO_2$.

Rh 3d XPS analysis of CeO_2-supported Rh catalysts

Figs. 3 and 4 show the Rh 3d XPS spectral analyses of all the eight Rh/CeO_2 catalyst samples via curve-fitting.

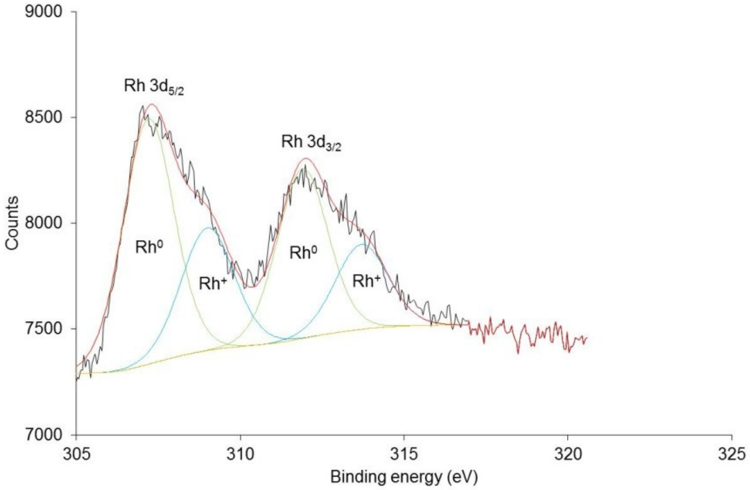

Fig. 3 Rh 3d XPS spectra of $Rh(N)/CeO_2$ obtained from $Rh^{3+}(N)/CeO_2$ calcined at 400 °C. The black and red curves stand for the raw experimental data and the sum of the Gaussian components, respectively.

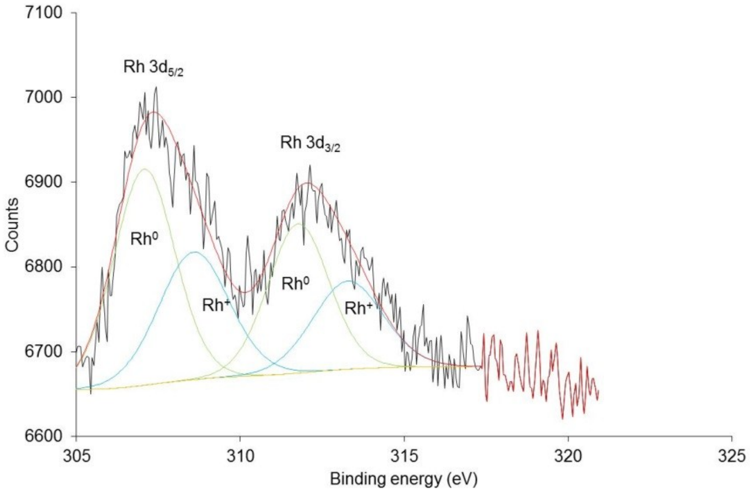

Fig. 4 Rh 3d XPS spectra of Rh(N)/CeO_2 obtained from Rh^{3+}(N)/CeO_2 calcined at 700 °C. The black and red curves stand for the raw experimental data and the sum of the Gaussian components, respectively.

XRD analysis of CeO_2-supported Rh catalysts

Figs. 5 and 6 show the XRD patterns of Rh(N)/CeO_2 and Rh(A)/CeO_2 before and after 25 h of ESR at 350 °C.

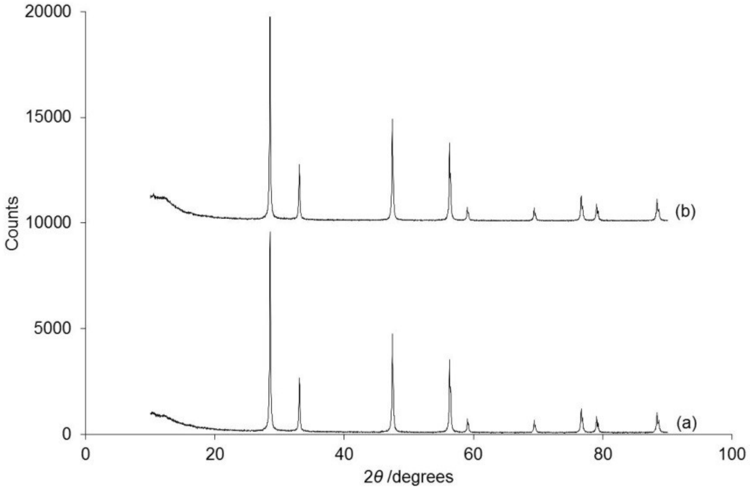

Fig. 5 XRD patterns of Rh(N)/CeO_2 (a) before and (b) after 25 h of ESR at 350 °C.

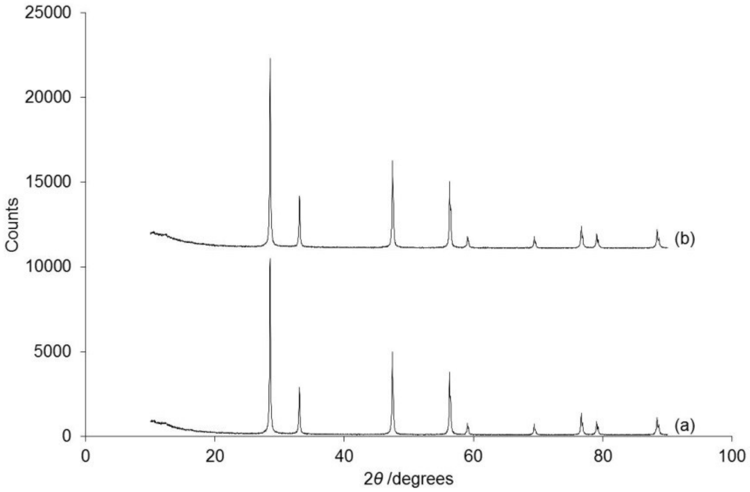

Fig. 6 XRD patterns of Rh(A)/CeO_2 (a) before and (b) after 25 h of ESR at 350 °C.